

Cite this: DOI: 00.0000/xxxxxxxxxx

Solvation in nitration of benzene and the valence electronic structure of Wheland intermediate[†]Kaho Nakatani,^a Sho Teshigawara,^a Yuta Tanahashi,^a Kento Kasahara,^{a,‡} Masahiro Higashi,^{a,b} and Hirofumi Sato^{*a,b,c}

Received Date

Accepted Date

DOI: 00.0000/xxxxxxxxxx

Nitration of benzene is a representative aromatic substitution reaction related to the σ -complex (arenium ion or “Wheland” intermediate) concept. This reaction is typically carried out in the mixed acid solution to generate nitronium ion, and how solvent molecules play roles in the reaction have been of great interest. Here we will shed new light on the reaction, namely the electronic structure and the microscopic insights of the solvation, which have been rarely discussed so far. We studied this process using the reference interaction site model-self consistent field with constrained spatial electron density distribution (RISM-SCF-cSED) method, considering sulfuric acid or water molecules as a solvent. In this method, the electronic structure of the solute and the solvation structure are self-consistently determined based on quantum chemistry and statistical mechanics of molecular liquids. The solvation free energy surfaces in solution and solvation structures were verified. In the bond formation process of benzene and nitronium ion, the solvation structure by sulfuric acid molecules drastically changes and solvation effects to the free energy is quite large. We revealed largely contributing resonance structures in the π -electron system of the σ -complex in gas and solution phases by analysing valence electronic structures.

1 Introduction

Electrophilic aromatic substitution is a textbook reaction in organic chemistry related to important chemical concepts such as aromatic selectivity.^{1,2} Many experimental and theoretical studies have been devoted to clarifying the process, and a reaction pathway via σ -complex (arenium ion or “Wheland” intermediate, as other names) is now established. Even in recent years, however, quests for their reaction mechanisms have not been exhausted.³ Recent theoretical studies for this topic have discussed the possible reaction pathways in which σ -complexes are not formed.^{4–7} The reaction path via σ -complex might be altered by substitution or environmental effects. The importance of dynamical effects for the selectivity⁸ or autocatalysis⁹ in some nucleophilic aromatic substitutions were also pointed out in connection with the solvent effects. It seems to be becoming clear that a critical factor

for the various mechanisms of these reactions is the effect of the surrounding environment.

Nitration of benzene is industrially essential and will be the most profoundly studied reaction among electrophilic aromatic substitutions both experimentally^{10–13} and theoretically (see, e.g. the review in Ref. [14]). The involvement of nitronium (NO_2^+) ion as a reactant is now widely recognised. In nitration, selecting solvents is essential,^{10–13} and a typical solvent is the mixed acid of concentrated sulfuric and nitric acids. A significant role of sulfuric acid is considered to protonate nitric acid molecules and make it easier to produce nitronium ions. It is also believed that the final step in the nitration of benzene involves deprotonation by solvent molecules such as H_2SO_4 to form nitrobenzene. In addition to this direct participation of solvent molecules, the whole free energy surface of this reaction is greatly affected due to the solvation. From computational aspects, however, the complexity of the solvent environment makes the treatment of the reaction very challenging.

Compared to the numerous theoretical studies for isolated molecular systems focusing on the mechanism of nitration and the analysis of electronic structures, the study of solvation effects has been very limited. The importance of proper modelling of solvation in this reaction was recently emphasised in Ref. [5]. Previous works with a polarisable continuum model

^a Department of Molecular Engineering, Graduate School of Engineering, Kyoto University, Nishikyo-ku, Kyoto 615-8510, Japan. E-mail: hirofumi@moleng.kyoto-u.ac.jp

^b Elements Strategy Initiative for Catalysts and Batteries (ESICB), Kyoto University, Nishikyo-ku, Kyoto 615-8520, Japan

^c Fukui Institute for Fundamental Chemistry, Kyoto University, Takano Nishihiraki-cho 34-4, Sakyo-ku, Kyoto 606-8103, Japan

[‡] Present Address: Division of Chemical Engineering, Graduate School of Engineering Science, Osaka University, Toyonaka, Osaka 560-8531, Japan

[†] Electronic Supplementary Information (ESI) available: [details of any supplementary information available should be included here]. See DOI: 00.0000/00000000.

(PCM)¹⁵ suggested that the solvation drastically changes the reaction profile of benzene nitration and affects the electronic structures.^{5,14,16–18} Despite these efforts, the reaction process as a chemical phenomenon in condensed molecular systems, especially the microscopic solvation, is still unknown. In the reaction process, the role of the typically mixed acid condition, or countless amounts of sulfuric acid molecules, has never been investigated.

In this work, we focus on the solvent effect and the electronic-structure change on benzene nitration. To the best of our knowledge, there have been no hybrid quantum-mechanical/molecular mechanics (QM/MM) studies on nitration reaction. The lack of these studies is presumably because adequate samplings in QM/MM simulations are still significant challenges for systems including ionic species, making it infeasible to compute the free energy profile of the reaction. A hybrid method between the statistical mechanics of molecular liquids,¹⁹ namely the reference interaction site model (RISM), and electronic structure theory is promising to overcome the difficulty. Here, we used the most sophisticated version, RISM-SCF-cSED (constrained spatial electron density distribution) method.^{20,21} This method can be regarded as an alternative to QM/MM but more efficient, capable of avoiding the sampling issue because of the algebraic nature of the RISM.²² A variety of similar methods^{23,24} are now following the same strategy. Another concern is the valence electronic structure of the σ -complex, which has been of interest to researchers.^{25–30} In electrophilic aromatic substitution reactions, aromatic stabilisation in the original six-membered ring is destroyed, and a σ -bonding is formed instead. The electronic origin of alternative stabilisation in the σ -complex is of great interest, and analyses based on resonance theory with quantitative calculations are desirable. *Ab initio* valence bond (VB) methods are powerful tools to tackle this issue, and an interesting explanation of substitution effects on electrophilic aromatic substitutions was discussed.²⁹ We applied the recently proposed scheme of analysis,³¹ briefly described in the next section, to reveal the valence π -electronic structure of the σ -complexes. Additionally, how solvation affects the electronic state is one of the issues, providing a way of qualitative understanding of the σ -complex. From these complementary perspectives, we intended to understand the process of nitration of benzene in solution.

The structure of this paper after this section is as follows. Computational details and the outline of theoretical methods used are described in **Section 2**. Assessment of free energy surfaces and solvation structures are reported, and chemical insights extracted from them are provided in detail in **Section 3**.

2 Methods

2.1 RISM-SCF method

A recent review of the RISM-SCF theory and its applications can be found elsewhere.²² Here we introduce a few basic quantities and terminologies for subsequent discussions.

Free energy in the RISM-SCF theory was evaluated as

$$A_{\text{RISM-SCF}} = E_{\text{solvated}} + \Delta\mu + E_{\text{tm}} \quad (1)$$

where E_{solvated} is the potential energy of the solute molecule, and $\Delta\mu$ is the excess chemical potential, or solvation free energy. The solvated Fock operator is derived using the extended variational principle³². E_{tm} represents thermal contributions. The solvation free energy in the hypernetted chain (HNC) approximation is represented as³³

$$\Delta\mu = -\rho k_{\text{B}} T \sum_{\alpha,s} \int d\mathbf{r} \left[c_{\alpha s}(r) - \frac{1}{2} h_{\alpha s}^2(r) + \frac{1}{2} h_{\alpha s}(r) c_{\alpha s}(r) \right] \quad (2)$$

where ρ , k_{B} and T are the density of the solvent, Boltzmann constant, and the temperature, respectively. The functions $c_{\alpha s}(r)$ and $h_{\alpha s}(r)$, depending on the position r , are called “direct” and “total” correlation functions for the atomic site α in the solute molecule and s in solvent molecules respectively, which can be obtained by solving the RISM equation so as to be consistent with the charge distribution in the solute molecule. Radial distribution function (RDF) representing the solvation structure is given as

$$g_{\alpha s}(r) = h_{\alpha s}(r) + 1. \quad (3)$$

2.2 Analysis of valence electronic structure

We are interested in the four electron π -valence electronic structure of the σ -complex. We outline the analysis method of valence electronic structures³¹ for the discussion in **Section 3.4**. This analysis is basically based on the mapping of molecular orbital (MO) type wave functions into resonance structures or VB type functions.³⁴ We start from the fact that any MO-based wave function Ψ can be represented as a linear combination of atomic spin orbital (ASO)-based determinants $\{\Psi_i^{\text{ASO}}\}$ as

$$\Psi = \sum_i K_i \Psi_i^{\text{ASO}} \quad (4)$$

where K_i is the expansion coefficient of i -th ASO-based determinant Ψ_i^{ASO} . Then, the weight w_i for the ASO-based determinant Ψ_i^{ASO} can be evaluated based on the definition of Chirgwin and Coulson³⁵ as

$$w_i = K_i \langle \Psi | \Psi_i^{\text{ASO}} \rangle. \quad (5)$$

Since ASOs are distributed on atomic sites, the weight of an ASO-determinant is identified as the weight of corresponding “resonance structure”. Here, the analysis method developed by us³¹ is used to evaluate w_i . For a single determinant case, the weight w of any ASO-determinant of the type of $|\chi_a^\alpha \chi_b^\alpha \chi_c^\beta \chi_d^\beta|$ where χ_μ^σ is the ASO (σ and μ are spin and special labels respectively) can be represented with σ -spin density matrices \mathbf{P}^σ and overlap matrix \mathbf{S} of the atomic orbital basis set as

$$w \left(|\chi_a^\alpha \chi_b^\alpha \chi_c^\beta \chi_d^\beta| \right) = \{ (\mathbf{P}^\alpha \mathbf{S})_{aa} (\mathbf{P}^\alpha \mathbf{S})_{bb} - (\mathbf{P}^\alpha \mathbf{S})_{ab} (\mathbf{P}^\alpha \mathbf{S})_{ba} \} \\ \times \{ (\mathbf{P}^\beta \mathbf{S})_{cc} (\mathbf{P}^\beta \mathbf{S})_{dd} - (\mathbf{P}^\beta \mathbf{S})_{cd} (\mathbf{P}^\beta \mathbf{S})_{dc} \}. \quad (6)$$

When extended basis sets are used, following weights in terms of atomic sites A , B , C and D are redefined and evaluated in the

similar manner to the population analysis.

$$\sum_{a \in A, b \in B, c \in C, d \in D} w \left(\left| \chi_a^\alpha \chi_b^\alpha \chi_c^\beta \chi_d^\beta \right| \right) \quad (7)$$

We call the above quantity “weight of resonance structure” corresponding to the ASO-based determinants. Hence, the present analysis can be applied to any wave functions based on the linear combination of atomic orbitals (LCAO) approximation, including the density functional theory. It is not always necessary to use valence bond or multiconfigurational self-consistent field methods, which are commonly employed in the analysis from the viewpoint of resonance structure. The present method has been used successfully to analyse the wave functions of various molecules, and the results showed good agreement with *ab initio* VB results.³¹

2.3 Computational details

Following previous considerations on basis sets and functionals,^{5,14,16,17} free energy surfaces for nitration of benzene were evaluated with the density functional method with the M06-2X³⁶ functional and 6-311G(d,p) basis set. At first, geometry optimisations in solution were performed with the conductor-like polarisable continuum model (CPCM)^{37,38} of the H₂O solution. The total free energy in the PCM was evaluated at the optimal structure as the sum of electrostatic, dispersion, repulsion, cavitation energies and contribution due to the thermal motions.

$$G_{\text{PCM}} = E_{\text{el}} + E_{\text{disp}} + E_{\text{rep}} + E_{\text{cav}} + E_{\text{tm}} \quad (8)$$

We evaluated E_{tm} as the zero-point energy (ZPE).

The RISM-SCF-cSED^{20,21} calculations were performed explicitly considering sulfuric acid solution, optimising geometries with its analytical energy gradient.³⁹ Though mixed solvents can be treated with the RISM, we considered pure solvent conditions to simplify the model. For aqueous solution, geometries optimised with the PCM were used for the RISM-SCF-cSED single-point calculations and E_{tm} in Eq. (1) was evaluated by the ZPE obtained with the PCM. The RISM equation was solved with the HNC approximation. Temperature was set to 298.15 K, and the densities 1.8255 g/cm³ (H₂SO₄) and 0.99705 g/cm³ (H₂O) based on the experimental data.⁴⁰ The molecular structure of H₂SO₄, as a solvent in the RISM, was determined by the geometry optimisation with M06-2X/6-311+G(2d,2p) imposing C₂ symmetry. Then, atomic electrostatic potential (ESP) charges were evaluated by CHELPG⁴¹ scheme. The atomic charges and Lennard-Jones (LJ) potential parameters are gathered in **Table 1**, mostly taken from the standard OPLS force field.^{42,43}

For the electronic structure analysis in **Section 3.4**, we used Pipek-Mezey procedure⁴⁴ to determine the valence electron spaces. This localisation procedure tends to preserve the σ/π -separation.⁴⁴ We note that the localisation of molecular orbitals does not affect the density matrix in the valence electron space if the π -orbital space is uniquely determined. Finally, the π -orbital space is extracted.

For the calculations with the RISM-SCF-cSED method and subsequent analysis of the valence electronic structures, we used the modified version of GAMESS⁴⁵ program. Other quantum chemi-

cal computations were conducted with Gaussian 16⁴⁶ program.

Table 1 Lennard-Jones parameters and atomic charges used in the RISM and RISM-SCF-cSED calculations.

	Atom	$\sigma/\text{\AA}$	$\epsilon/\text{kcal mol}^{-1}$	Charge
Nitro moiety	N	3.250	0.120	–
	O	2.960	0.170	–
Benzene moiety	C	3.550	0.070	–
	H	2.420	0.030	–
H ₂ SO ₄ , H ₃ SO ₄ ⁺	S	3.550	0.250	1.05712 ^c
	O(=)	2.960	0.210	–0.44478 ^c
	O	3.000	0.170	–0.51862 ^c
H ₂ O ^a	H ^b	1.000	0.056	0.43484 ^c
	O	3.166	0.155	–0.82
	H ^b	1.000	0.056	0.41

^aSPC-like model. ^bWe followed the convention for the parameters of proton in OH-groups. ^cCharges used for H₂SO₄.

3 Results and discussions

3.1 Liquid structure of H₂SO₄ solution

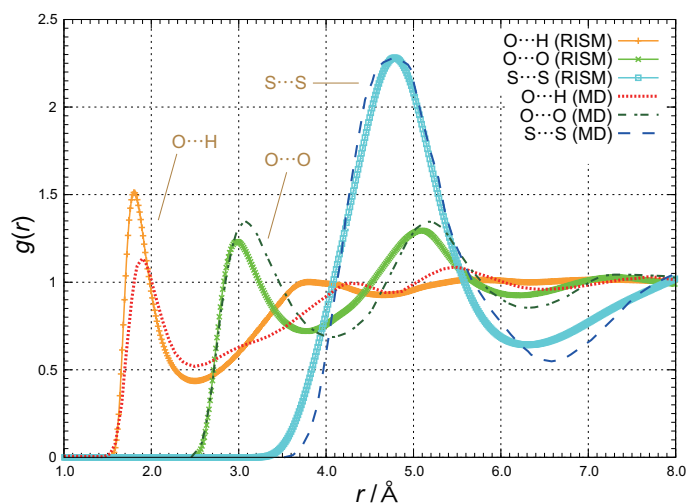


Fig. 1 Radial distribution functions for O(=)⋯H, O(=)⋯O(=) and S⋯S in the H₂SO₄ solution obtained with the RISM. The results by the MD simulation at 298 K⁴⁷ are included for comparison.

The RDFs for the H₂SO₄ solution obtained by the RISM is shown in **Figure 1**, compared with those with the molecular dynamics (MD) simulation at 298 K.⁴⁷ Although the employed LJ-parameters of the hydrogen atom in the hydroxyl group are slightly different, the RDFs computed with these two methods show excellent agreement, particularly for O(=)⋯O(=) and S⋯S. These results indicate that RISM theory adequately describes the liquid structure of the H₂SO₄ solution.

3.2 Free energy surfaces

The free energy profile for nitration of benzene in solution phases computed with the RISM-SCF-cSED is shown in **Figure 2**. The profile in the gas phase (sum of potential energy and ZPE) and the profile calculated with PCM are also included in the figure for comparison. The molecular structures at energy minimum in the gas phase and solution are also illustrated.

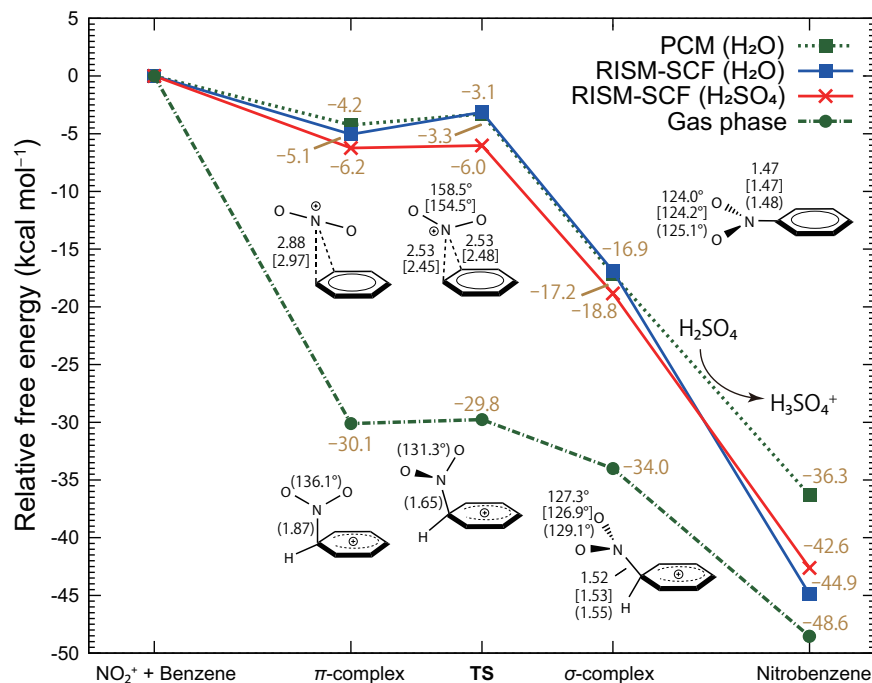


Fig. 2 Relative free energies (kcal mol⁻¹) in nitration of benzene in gas and solution phases. Solution phase conditions were modeled with the RISM-SCF-cSED (H₂SO₄ and H₂O solvent) and with the PCM (H₂O solvent). Schematic molecular structures are included with some important structural parameters (bond lengths in Å and bond angles in degree) for gas phase (in parenthesis), for solution phases modeled by the PCM (in bracket) and RISM-SCF-cSED.

Consistent with previous theoretical computations (e.g. Ref. [49]), our calculations found many energy minima on the reaction energy surface. Here, we considered one possible energy minimum structure, connecting to the σ -complex through the transition state (TS). We call this precursor of the σ -complex as “ π -complexes” in the present study. In the gas phase, all three structures relatively resemble each other, and the N–C bond is less than 2.0 Å, even at the early stage of the reaction. The early strong-bond formation is consistent with the high stabilisation of π -complexes.

On the other hand, the π -complex and TS structures in the solution phase are very different from those in the isolated system and somewhat like weak aggregates of nitronium ion and benzene. The N–C distances are much longer, and the free energy surface around the π -complex is flat. We confirmed that TS is connecting to the energy minimum structures, π - and σ -complexes, by subsequent structure optimisations along with the imaginary vibrational mode. The structures of π -complex and TS varied depending on the solvation models, but the difference was insignificant.

Despite the entirely different theoretical foundations, the RISM-SCF-cSED (H₂SO₄ or H₂O solutions) and PCM give similar results for the overall energy profile except for the final product. Presumably, this similarity is attributed to the +1 total charge of the system. The strong electrostatic interaction between the solute and solvent primary determines the energy profile. At the same time, because of the large size, the electrostatic field generated by the solute molecules is small, and specific solvation such as hydrogen bonding is rarely formed. The oxygen atoms con-

stituting water or H₂SO₄ are negatively charged and coordinate directly to the solute molecules. As we will see later, however, the peak of the radial distribution function is not very high. Although the agreement between the two solvation models is not self-evident, such similarity is often observed.⁴⁸ The free energies at the π -complex and TS are comparable (within 2 kcal mol⁻¹ difference) in the solution phases, suggesting the π -complex is not stable. Our results agree with the fact that experimental observation of the stable π -complex is difficult.¹⁶ In the gas phase, π -complexes were formed and considerably stabilised. This stabilisation can be attributed to the instability of nitronium ions.

In the final step, we assumed the deprotonation of the σ -complex by H₂SO₄ molecule, which is the most abundant species in the solution system (σ -complex + H₂SO₄ → nitrobenzene + H₃SO₄⁺).¹⁶ Though the free energy change by deprotonation in the H₂SO₄ solution was evaluated as -23.8 kcal mol⁻¹ as shown in the figure, deprotonation by other solvent molecules will be possible in the real experimental condition. As an example, stabilisation due to the abstraction by HSO₄⁻ anion was -60.5 kcal mol⁻¹. Based on the equilibrium constant, the amount of the anion is much smaller than that of H₂SO₄, but the change in the deprotonation could be lower than -23.8 kcal mol⁻¹ in the real condition of solution. Nitrobenzene, the final product, is neutral species and de-solvated (we will see later). It could also be easily protonated in the solution. Intramolecular proton migration could occur to form protonated nitrobenzene in the gas phase,^{49,50} though this path would be far from the main path in solution because deprotonations from the σ -complex or the isomers formed via proton migration could occur with a very low or

no barrier.

For the H₂O solution, the comparison between RISM-SCF-cSED and PCM is possible, and the largest difference in the free energy change (8.6 kcal mol⁻¹) is observed in the final step. As shown in **Electronic Supplementary Information**, the difference in the solvation energy change on nitrobenzene is 20.87 kcal mol⁻¹, which may be attributed to the importance of hydrogen bonding as mentioned above. The stabilisation by the protonation of H₂SO₄ is evaluated more largely in PCM than in RISM-SCF-cSED in terms of solvation energy (-13.27 kcal mol⁻¹). Hence, together with the contribution from the polarisation of the electronic structure (about 1 kcal mol⁻¹), 8.6 kcal mol⁻¹ is evaluated.

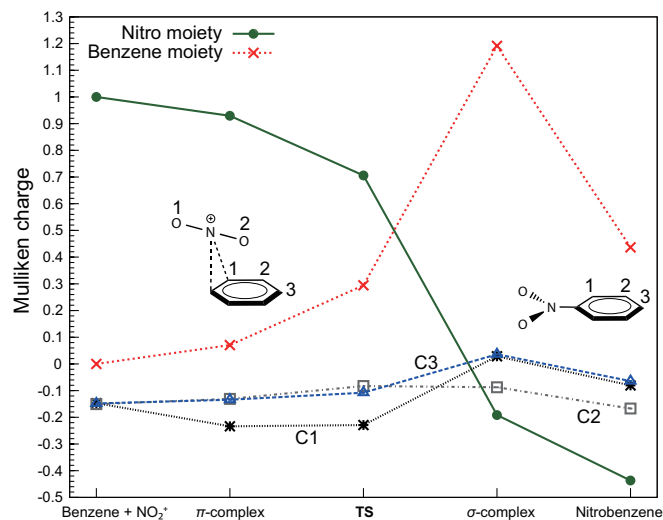


Fig. 3 Changes of Mulliken charges in the nitro (NO₂) and benzene moieties, and on the C1, C2 and C3 carbon in the benzene moiety calculated with the RISM-SCF-cSED (H₂SO₄ solvent) along the reaction coordinate. Charge of the moiety means sum of atomic charges in the domains. Numbering of atoms are included in the figure.

3.3 Solvation structures and solvation free energies

We firstly show the changes of Mulliken charges in the process of nitration obtained with the RISM-SCF-cSED for the H₂SO₄ solvent in **Figure 3**. As the reaction proceeds, charge transfer occurs from the benzene moiety to the nitro moiety. The significant changes of Mulliken charges in these moieties are observed, and the transfer roughly corresponding to one electron occurs from the reactant to σ -complex. We can also see that the C1 and C3 carbons tend to gain the positive charge in the σ -complex whilst the C2 carbon remains negatively charged.

Changes in the electronic and solvation structures are closely related. The RDFs for the reaction system and H₂SO₄ solvent molecules obtained with the RISM-SCF-cSED method are shown in **Figure 4**. As can be seen from figures (a) and (b), remarkable changes of solvation structures around the nitrogen atoms are observed in the reaction process. Along with the change of electronic structure, the first sharp peak of $g_{\text{NO}}(r)$ at 3.0 Å for the nitronium ion gradually decreases, and its shoulder peak around 3.7 Å rises and shifts to 4.0 Å in the σ -complex. The peaks of $g_{\text{NS}}(r)$ at 4.2 Å for the nitronium ion or the π -complex becomes

broad, descends and recedes to 4.5 Å in the σ -complex or nitrobenzene. Summarising these changes in RDFs, the evolution of the coordination along the reaction can be depicted in **Figure 5**. For nitronium ion or the π -complex, sulfuric acid molecules tend to coordinate strongly with an oxygen atom. In the σ -complex or nitrobenzene, sulfuric acid molecules tend to coordinate weakly with one or two oxygen atoms. From the geometrical considerations on 1.42 Å of S=O bond length, the angle between the nitrogen atom and O(=) and S atoms of a sulfuric acid molecule ($\angle\text{NOS}$) in the first solvation shell is estimated as 143° and 103° in the π - and σ -complexes, respectively. **Figures 4 (c) and (d)** are solvation structures around the *para*-carbon atom, C3 (see **Figure 3** for the numbering). At first, both $g_{\text{CO}}(r)$ and $g_{\text{CS}}(r)$ are the lowest in benzene and raised to the highest in the σ -complex, consistent with the fact that C3 carbon is positively charged. However, the heights of peaks are lower than those for hetero atoms. **Figure 4 (e)** shows that sharp peaks at 1.8 Å in $g_{\text{OH}}(r)$ are detected for σ -complex and nitrobenzene. Namely, the conspicuous hydrogen bonding is formed around the nitro moiety. At first, there is no hydrogen bonding around the cation, but the peak becomes rapidly higher along with the N-C bond formation, responding to the change in the electronic structure of the moiety.

The solvation free energies $\Delta\mu$ in the process of nitration in H₂SO₄ solution are shown in **Figure 6**. The system gains the most considerable stabilisation by solvation at the beginning of the reaction, where benzene and nitronium ion are separated. Stabilisation by solvation depends on the electronic state of the solute molecule. At TS, the positive charge is delocalized over benzene and nitronium ion moieties and $\Delta\mu$ at the structure increase (destabilised) compared with those at the π - or σ -complexes. The results also show that nitrobenzene has positive solvation free energy (+12.6 kcal mol⁻¹) in the H₂SO₄ solution. This apparent destabilisation by solvation in nitrobenzene is compensated by gaining negatively large $\Delta\mu$ by H₃SO₄⁺. Solvation free energies for H₃SO₄⁺ and H₂SO₄ were evaluated as -67.7 kcal mol⁻¹ and -15.6 kcal mol⁻¹, respectively.

3.4 Valence electronic structure of σ -complex

π -Valence electronic structure of σ -complex was analysed with resonance theory. Preliminarily, we confirmed that around 95% of MO coefficients are distributed on the C1-C5 carbons in the σ -complex (see **Figure 7** for the numbering) in two specific MOs considered in the present π -orbitals analysis.

π -Electron systems in the benzene and the nitro moieties are not conjugated. Valence electrons are assumed to be constructing the 5-center-4 π -electron systems (four electrons are distributed on the C1-C5 carbon atoms), which can be represented as the resonance structures shown in **Figure 8**. All resonance structures considered in our analysis are shown with their structural degeneracies in the parenthesis. Each structure has a corresponding ASO-determinant or linear combination of ASO-determinants. Single bonding in these structures represents singlet-coupling. Nine structures are covalent types (with one positive charge in the structure), sixteen are mono-ionic (with two positive and one negative charges) and six are di-ionic (with three positive and two

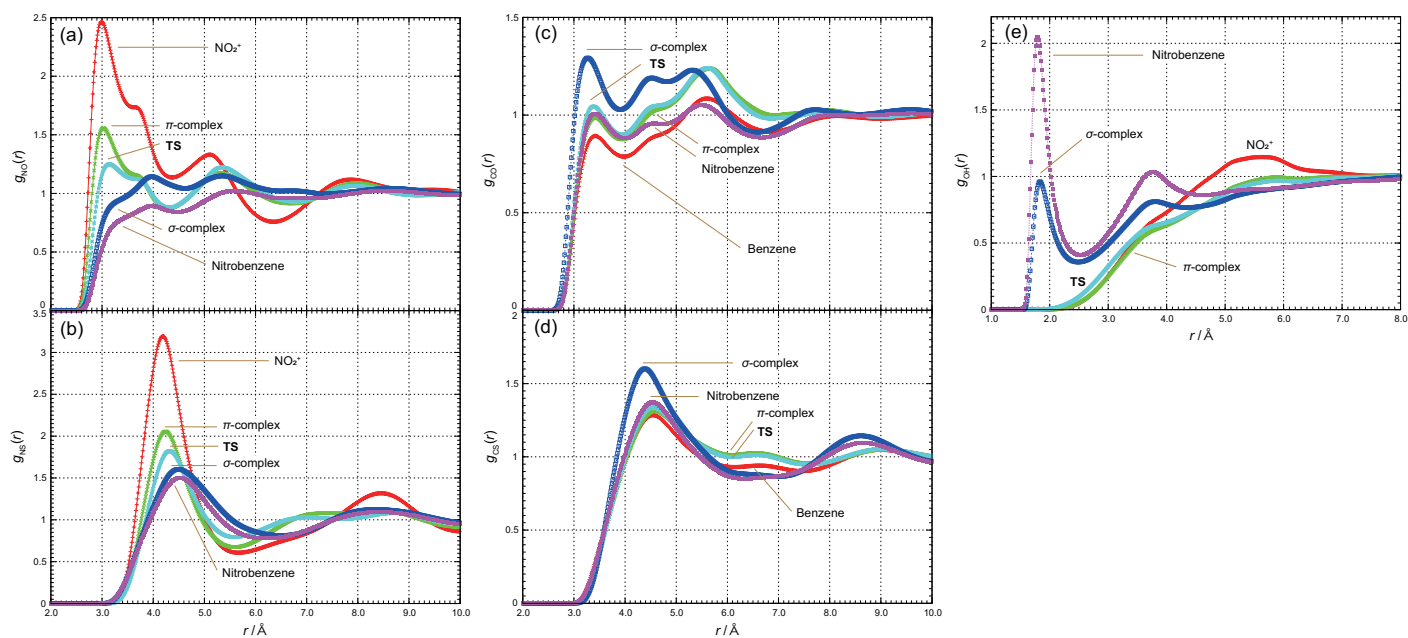


Fig. 4 Radial distribution functions for the nitration reaction system (nitro and benzene moieties) and H_2SO_4 solvent molecules: (a) $\text{N}\cdots\text{O}(=)$, (b) $\text{N}\cdots\text{S}$, (c) $\text{C}3\cdots\text{O}(=)$, (d) $\text{C}3\cdots\text{S}$ and (e) $\text{O}1\cdots\text{H}$. See **Figure 3** for the numbering of carbon and oxygen atoms.

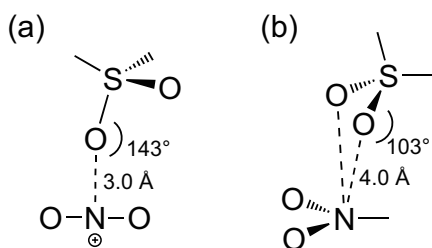


Fig. 5 Schematic representation of representative coordination structures of sulfuric acid molecules (a) for the π -complex and (b) for the σ -complex. Important structural parameters which were estimated from the RDFs of the π - and σ -complexes are included.

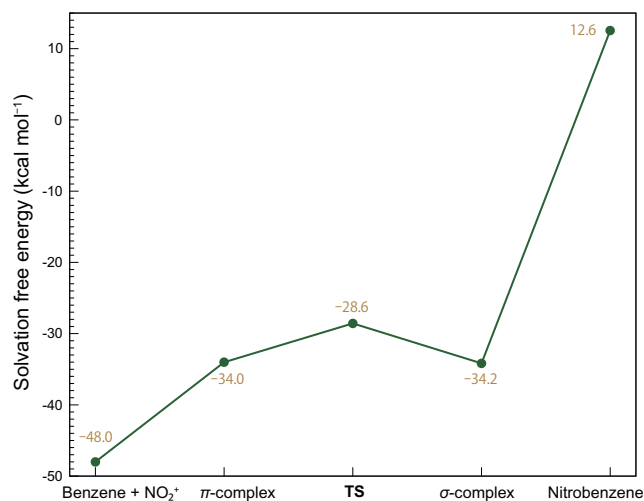


Fig. 6 Solvation free energies $\Delta\mu$ (kcal mol⁻¹) in the process of nitration of benzene in the H_2SO_4 solution modeled with the RISM-SCF-cSED.

negative charges). Solvation effects were also verified with the RISM-SCF-cSED and PCM. The structure optimised by the PCM was used for the analysis.

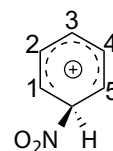


Fig. 7 Numbering of carbon atoms in the σ -complex.

The computed weights of resonance structures are gathered in **Figure 9 (a)**. We found that the weight of the structure **13** are especially large in the σ -complex (14.44%). In this structure, a negative charge is surrounded by two positive charges. This observation suggests that the resonance of these structures contributes largely to the stabilisation. The delocalized structures such as **1**, **3**, **4**, **7** and **9** have also large weights and positive charges tend to distributed on the C3 position. As can be seen from the figure, the solvation effect on the weights was small. That will become clearer when compared with the substitution effects. Results of the analysis for benzenium ion and nitro-substituted one are provided in **Electronic Supplementary Information**. Weights evaluated with other exchange-correlation functionals are also included there. The functional dependence was not so significant as far as we tested. The present results cannot directly be compared with those by Hadzic et al.²⁹ computed with *ab initio* VB because their VB basis does not explicitly include ionic structures. Nevertheless, positively charged C1 and C3 sites are consistent with their results.

We discuss the solvation effects on the valence electronic structure in more detail. Changes of weights due to the solvation are shown in **Figure 9 (b)** for the ease of reading. Generally, some

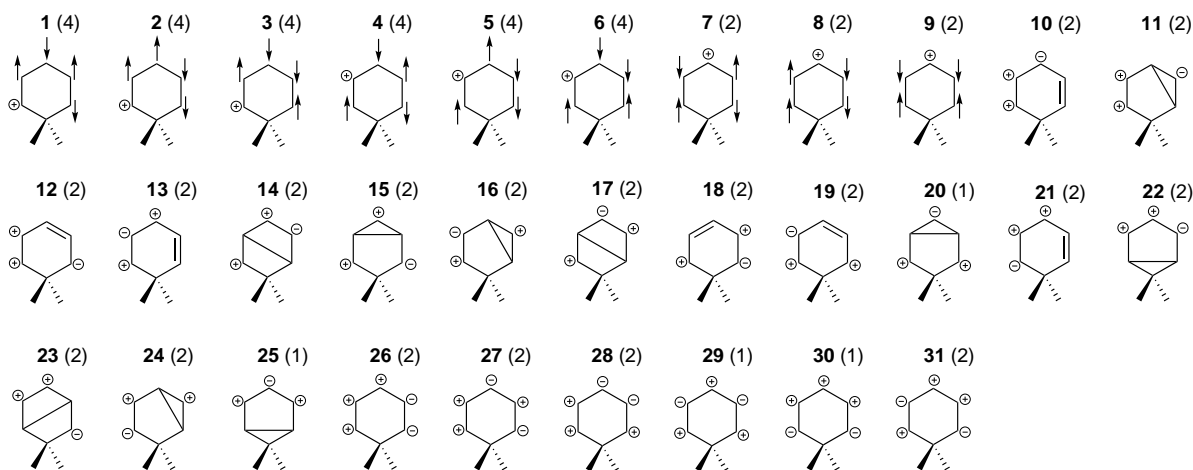


Fig. 8 All the resonance structures of σ -complex considered in the analysis of π -valence electronic structure. Structural degeneracies are given in parentheses.

preferable ionic structures are expected to be emphasized by the solvation. In fact, the structures whose weights relatively largely increased are **7**, **9**, **13**, **21** and **31**, and the positive charge on the C3 carbon is slightly emphasized by solvation. However, the weight change due to the solvation was generally not so large and less significant than the substitution. These results are attributed to the cationic character of σ -complex, namely, the electronic structure is tight enough, being insensitive to the electric field generated by the solvent environment.

4 Conclusion

In the present study, we verified the process of nitration of benzene, considering the sulfuric acid and aqueous solution environments with the RISM-SCF-cSED method. New insights are summarized as follows.

Significant solvation effects on the free energy surface contain the consequences of the reorganisation of the solvation structure. The changes of the solute molecule's electronic state accompany the solvation structure changes by H_2SO_4 . In the formation of the σ -complex, charge transfer from the benzene moiety to the nitrogen atom occurs. Before the charge transfer, sulfuric acid molecules relatively strongly coordinate to the nitrogen atom in the nitro moiety with an oxygen atom. In the σ -complex or nitrobenzene, on the other hand, sulfuric acid molecules tend to coordinate weakly. We also provided the unique solvation structure around the σ -complex. Additionally, π -valence electronic structures of σ -complexes were analyzed, and dominant resonance structures were identified. We found that the resonance structure in which a negative charge is surrounded by two positive charges largely contributes to the valence electronic structure of the σ -complex. Unlike substitution effects, solvation does not largely change the valence state due to the robust electronic structure of the cationic species. These findings will give a qualitative understanding of the electronic structure of σ -complexes.

Conflicts of interest

There are no conflicts to declare.

Acknowledgements

KN is thankful for the Grant-in-Aid for the Japan Society for Promotion of Science (JSPS) Fellows. This work was supported by the JSPS KAKENHI (Grant No. JP20J23328, JP17H03009 and JP20H05839). The management of Elements Strategy Initiative for Catalysts and Batteries (ESICB) is also acknowledged. Theoretical computations were partly performed using the Research Center for Computational Science, Okazaki, Japan.

Notes and references

- 1 G. W. Wheland, *Resonance in Organic Chemistry*, Wiley, New York, 1955.
- 2 J. Clayden, N. Greeves and S. Warren, *Organic Chemistry*, 2nd ed., Oxford University Press, New York, 2012.
- 3 J. Mortier, Ed., *Arene Chemistry: Reaction Mechanism and Methods for Aromatic Compounds*, Wiley, New York, 2016.
- 4 B. Galabov, G. Koleva, S. Simova, B. Hadjieva, H. F. Schaefer III and P. v. R. Schleyer, *Proc. Natl. Acad. Sci. U.S.A.*, 2014, **111**, 10067–10072.
- 5 B. Galabov, D. Nalbantova, P. v. R. Schleyer and H. F. Schaefer III, *Acc. Chem. Res.*, 2016, **49**, 1191–1199.
- 6 T. Stuyver, D. Danovich, F. De Proft and S. Shaik, *J. Am. Chem. Soc.*, 2019, **141**, 9719–9730.
- 7 T. Stuyver and S. Shaik, *J. Am. Chem. Soc.*, 2021, **143**, 4367–4378.
- 8 Y. N.-Quinones and D. A. Singleton, *J. Am. Chem. Soc.*, 2016, **138**, 15167–15176.
- 9 R. V. Lommel, S. L. C. Moors and F. De Proft, *Chem. Eur. J.*, 2018, **24**, 7044–7050.
- 10 P. B. D. De La Mare and J. H. Ridd, *Aromatic Substitution: Nitration and Halogenation*, Butterworths Scientific Publications, London, 1959.
- 11 C. K. Ingold, *Structure and mechanism in organic chemistry*, 2nd Ed., Cornell University Press, New York, 1969.
- 12 G. A. Olah, *Acc. Chem. Res.*, 1971, **4**, 240–248.
- 13 J. H. Ridd, *Acc. Chem. Res.*, 1971, **4**, 248–253.

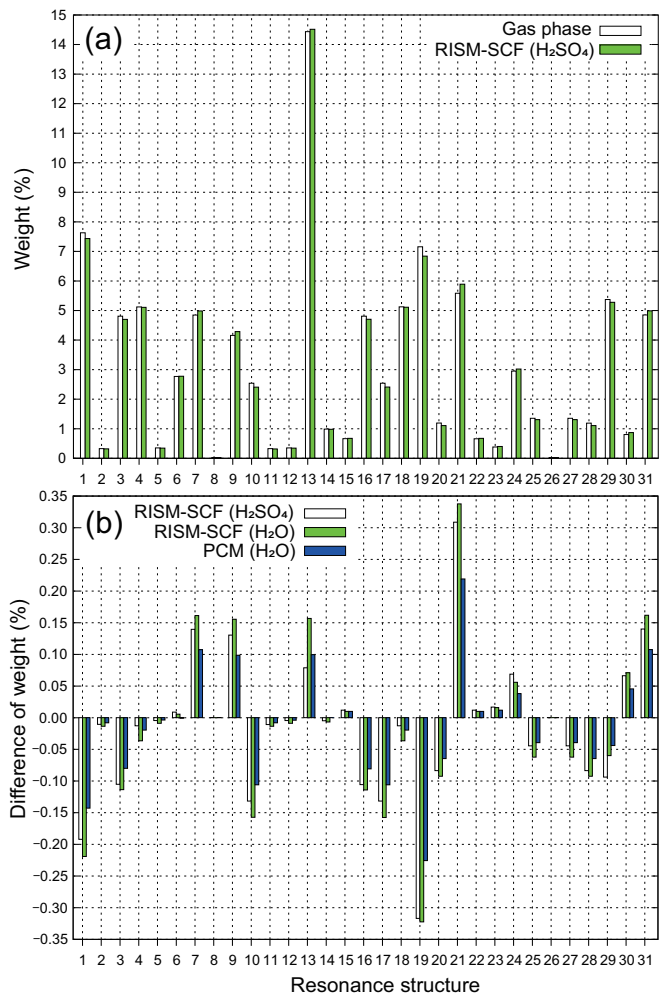


Fig. 9 (a) Weights of resonance structures in σ -complex in the gas and H_2SO_4 solution phases modeled with the RISM-SCF-cSED. (b) Differences of the weights in the solution modeled with the RISM-SCF-cSED (H_2SO_4 and H_2O) and with the PCM (H_2O) from weights in the gas phase.

14 T. Brinck and M. Liljenberg, in J. Mortier Ed., *Arene Chemistry: Reaction Mechanism and Methods for Aromatic Compounds*, 2016, Wiley, New York, pp. 83–105.

15 B. Mennucci and R. Cammi, Ed., *Continuum Solvation Models in Chemical Physics: From Theory to Applications*, Wiley, New York, 2007.

16 G. Koleva, B. Galabov, B. Hadjieva, H. F. Schaefer III and P. v. R. Schleyer, *Angew. Chem. Int. Ed.*, 2015, **54**, 14123–14127; *ibid.*, 2020, **59**, 7986–7986.

17 M. Liljenberg, J. H. Stenlid and T. Brinck, *J. Mol. Model.*, 2018, **24**:15.

18 L. Chen, H. Xiao, J. Xiao and X. Gong, *J. Phys. Chem. A*, 2003, **107**, 11440–11444.

19 J.-P. Hansen and I. R. McDonald, *Theory of Simple Liquids: with Applications to Soft Matter*, 4th ed., 2013, Elsevier, Boston.

20 D. Yokogawa, H. Sato and S. Sakaki, *J. Chem. Phys.*, 2007, **126**, 244504.

21 D. Yokogawa, *Chem. Phys. Lett.*, 2013, **587**, 113–117.

22 H. Sato, *Phys. Chem. Chem. Phys.*, 2013, **15**, 7450–7465.

23 Q. Du and D. Wei, *J. Phys. Chem. B*, 2003, **107**, 13463–13470; Q. Du, D. Beglov, D. Wei and B. Roux, *J. Phys. Chem. B*, 2007, **111**, 13658.

24 T. Kloss, J. Heil and S. M. Kast, *J. Phys. Chem. B*, 2008, **112**, 4337–4343.

25 S. R. Gwaltney, S. V. Rosokha, M. Head-Gordon and J. K. Kochi, *J. Am. Chem. Soc.*, 2003, **125**, 3273–3283.

26 N. Stamenković, N. P. Ulrih and J. Cerkovnik, *Phys. Chem. Chem. Phys.*, 2021, **23**, 5051–5068.

27 A. Arrieta and F. P. Cossi, *J. Mol. Struct. (Theochem)*, 2007, **811**, 19–26.

28 E. Kleinpeter and A. Koch, *J. Phys. Chem. A*, 2019, **123**, 4443–4451.

29 M. Hadzic, B. Bräida and F. Volatron, *Org. Lett.*, 2011, **13**, 1960–1963.

30 G. Raos, L. Astorri, M. Raimondi, D. L. Cooper, J. Gerratt and P. B. Karadakov, *J. Phys. Chem. A*, 1997, **101**, 2886–2892.

31 K. Nakatani, M. Higashi, R. Fukuda and H. Sato, *J. Comput. Chem.*, 2021, **42**, 1662–1669.

32 H. Sato, F. Hirata and S. Kato, *J. Chem. Phys.*, 1996, **105**, 1546–1551.

33 A. D. McLean and G. S. Chandler, *J. Chem. Phys.*, 1980, **72**, 5639–5648.

34 P. C. Hiberty and C. Leforestier, *J. Am. Chem. Soc.*, 1978, **100**, 2012–2017.

35 B. H. Chirgwin and C. A. Coulson, *Proc. Roy. Soc. Lond. Ser. A*, 1950, **201**, 196–209.

36 Y. Zhao and D. G. Truhlar, *J. Phys. Chem.*, 2006, **110**, 5121–5129.

37 V. Barone and M. Cossi, *J. Phys. Chem. A*, 1998, **102**, 1995–2001.

38 M. Cossi, N. Rega, G. Scalmani and V. Barone, *J. Comput. Chem.*, 2003, **24**, 669–681.

39 D. Yokogawa, H. Sato and S. Sakaki, *J. Chem. Phys.*, 2009, **131**, 214504.

40 The Chemical Society of Japan, Ed., *Handbook of Chemistry: Pure Chemistry II, 4th ed.*, 1993, Maruzen, Tokyo.

41 C. M. Breneman and K. B. Wiberg, *J. Comput. Chem.*, 1990, **11**, 361–373.

42 W. L. Jorgensen, D. S. Maxwell and J. T.-Rives, *J. Am. Chem. Soc.*, 1996, **118**(45), 11225–11236.

43 M. L. P. Price, D. Ostrovsky and W. L. Jorgensen, *J. Comput. Chem.*, 2001, **22**, 1340–1352.

44 J. Pipek and P. G. Mezey, *J. Chem. Phys.*, 1989, **90**, 4916–4926.

45 M. W. Schmidt, K. K. Baldrige, J. A. Boatz, S. T. Elbert, M. S. Gordon, J. H. Jensen, S. Koseki, N. Matsunaga, K. A. Nguyen, S. J. Su, T. L. Windus, M. Dupuis and J. A. Montgomery, *J. Comput. Chem.*, 1993, **14**, 1347–1363.

46 M. J. Frisch, G. W. Trucks, H. B. Schlegel, G. E. Scuseria, M. A.

- Robb, J. R. Cheeseman, G. Scalmani, V. Barone, G. A. Peters-
son, H. Nakatsuji, X. Li, M. Caricato, A. V. Marenich, J. Bloino,
B. G. Janesko, R. Gomperts, B. Mennucci, H. P. Hratchian, J.
V. Ortiz, A. F. Izmaylov, J. L. Sonnenberg, D. Williams-Young,
F. Ding, F. Lipparini, F. Egidi, J. Goings, B. Peng, A. Petrone, T.
Henderson, D. Ranasinghe, V. G. Zakrzewski, J. Gao, N. Rega,
G. Zheng, W. Liang, M. Hada, M. Ehara, K. Toyota, R. Fukuda,
J. Hasegawa, M. Ishida, T. Nakajima, Y. Honda, O. Kitao, H.
Nakai, T. Vreven, K. Throssell, J. A. Montgomery, Jr., J. E. Per-
alta, F. Ogliaro, M. J. Bearpark, J. J. Heyd, E. N. Brothers, K.
N. Kudin, V. N. Staroverov, T. A. Keith, R. Kobayashi, J. Nor-
mand, K. Raghavachari, A. P. Rendell, J. C. Burant, S. S. Iyen-
gar, J. Tomasi, M. Cossi, J. M. Millam, M. Klene, C. Adamo,
R. Cammi, J. W. Ochterski, R. L. Martin, K. Morokuma, O.
Farkas, J. B. Foresman, and D. J. Fox, Gaussian 16, Revision
B.01, Gaussian, Inc.: Wallingford, CT, 2016.
- 47 M. Canales and E. Guàrdia, *J. Mol. Liq.*, 2016, **224**, 1064–
1073.
- 48 H. Sato and S. Sakaki, *J. Phys. Chem. A*, 2004, **108**, 9, 1629
–1634.
- 49 P. M. Esteves, J. W. de M. Carneiro, S. P. Cardoso, A. G. H.
Barbosa, K. K. Laali, G. Rasul, G. K. S. Prakash and G. A. Olah,
J. Am. Chem. Soc., 2003, **125**, 4836–4849.
- 50 V. D. Parker, T. Kar and D. Bethell, *J. Org. Chem.*, 2013, **78**,
9522–9525.

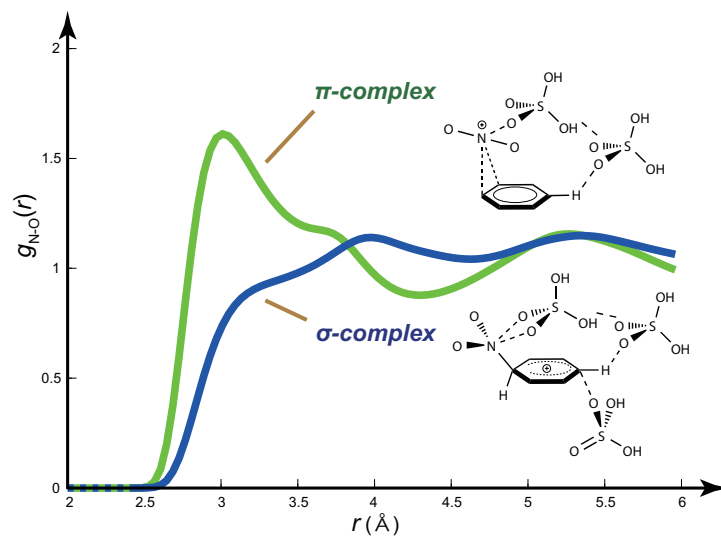


Fig. 10 Nitration of benzene was studied with the reference interaction site model-self consistent field (RISM-SCF) method, considering the sulfuric acid solvent. In the process of the bond formation between benzene and nitronium ion, the solvation structure drastically changes due to the charge transfer.